Application of non-destructive evaluation and signal processing for diagnosis of historic heritage buildings

J. Gosalbez, A. Salazar, G. Safont, I. Bosch, R. Miralles, L. Vergara, V. Albert
Instituto de Telecomunicaciones y Aplicaciones Multimedia,
Universitat Politècnica de València,
8G Building - access D - Camino de Vera s/n - 46022 Valencia (Spain)
Corresponding author: jgcastillo@dcom.upv.es

Abstract

In this work, signal processing techniques are combined with non-destructive evaluation (NDE) to evaluate the capability for detecting defects in historic walls. To join this aim, ashlar masonry walls of 3x2x0.2m have been made at laboratory facilities with controlled and localized defects. These scale walls have been inspected by means ultrasound and ground penetrating radar (GPR) with loads of different weights (0Tn, 10Tn, 50Tn and 80Tn). The ultrasonic and GPR signals provided tomographies that have been improved by means processing techniques. Related to ultrasonic tomographies, kriging algorithm have been implemented for visualization improvement. By the other hand, novelty differential tomographies have demonstrated their sensibility to defects. Related to GPR, different algorithms have been developed to improve the tomographies: elimination of the background noise, depth resolution enhancing and automatic detection and correction of hyperbolas due to radiation pattern of the antenna. Finally, it is concluded the added value of signal processing applied to NDE for the detection of defects in historic walls.

1. Introduction

Great part of the constructed heritage in our cities is built using stone and mortar, as well as brick as constitutive materials. This kind of constructions resists well the passage of time, nonetheless, degradation processes are inevitable [1][2] and difficulties exist when it is necessary to evaluate the degree of the above mentioned processes. The degradation processes affect so much structural level (cracks, fissures, detachments, displacements…) as aesthetic (dirt, crusts, efflorescence…) of the historical buildings. The knowledge of this reality will be important for the valuation of its stability conditions and also for restoration planning environment. The main pathologies that can result in the breakdown of historical buildings are humidity damages caused by capillarity ascent, breeze or high humidity environments, successive freeze-thaw cycles that result in crystallization, broken mortar joints, loss of the most exposed material and finally erosion damages caused by lack of vegetation.

Centering on structural pathologies (cracks, fissures …), the detection and characterization of the above mentioned problems is important to

Non–destructive evaluation techniques can be combined with signal processing algorithms from the perspective of diagnosis

estimate the state and to plan its possible repair. At present, to deal with this valuation, it is usual to realize destructive testing by means of the extraction and characterization of tubes from the material, principally stone tubes. These tubes are characterized using classical morphological and physiochemical analyses. Thus, physical-mechanical properties of the materials can be determined: one-axial compressive strength, water absorption, saturation, porosity, dimensional variation by temperature and humidity, salt crystallization strength, and damp-drying cycle [3] [4]. But the realization of these extractions supposes a degradation of the historic element and it only offers punctual information from the extraction position. Taking into account this limitation and that it is necessary to preserve to the maximum the integrity of the element due to the historic and cultural value, the detection should be as least invasive as possible. As far as possible, NDE should be used, like ultrasounds, X-rays, GPR, acoustic monitoring… This kind of tests do not alter the examined element, allow an analysis of the totality of the historic element and help to the valuation of the condition of the element and to choice the intervention-restoration technologies. Additionally, they can provide information after the repair.

NDEs are based on indirect measures [5], for this reason, it is necessary the utilization of different algorithms capable of extracting the information of the signals obtained from inspected material. For example, sonic and ultrasonic technologies are based on elastic or mechanical waves that propagate through the structure, whereas the exploration with GPR is based in the propagation and interpretation of electromagnetic waves. Both technologies measure the variations of the transmitted signals that are due to the interaction with the element under analysis. It is expected that these variations could be correlated with physical parameters: cracks, fissures, changes of properties… On the one hand, the technologies based on elastic waves are sensitive to the geometry of elements that compose the structure and to tensional condition of the same ones. On the other hand, the electromagnetic technologies are sensitive to the geometry and disposition of elements. Other NDE technologies as vision testing allow monitoring superficial parameters of deformation and displacement whereas X-rays testing allows detecting densities changes inside of materials.

When defects of the structural elements are detected (flaws, cracks that decrease compression resistance, break resistance to, deformation module…), it should be necessary the restoration and it will be useful to check the scope of the restoration tasks. For example, in case of sealed cracks and hollows by means of the injection of resins, it will be useful to evaluate the degree of penetration and consolidation because this degree will condition the improvement of the physical characteristics and the future degradation of material. NDE can again avoid a new deterioration on the restored material as well as the possibility to test the whole element because of preventing the extraction of probes.

The utilization of NDE already supposes an innovation in the area of the restoration, but the application of signal processing algorithm to this area will provide an added value and supposes a novelty technological advance in the process of evaluation of the historic and artistic heritage.

The objective of this paper is to combine NDE with signal processing algorithms from the perspective of diagnosis. The NDE selected have been ultrasounds and GPR. The present paper is organized as follows. In Section 2, the construction, dimensions and controlled defects of a scale ashlar masonry wall are described. This scale wall is analyzed by means different NDE and the results are compare with its known and real status. This Section 3 is dedicated to ultrasound testing. An introduction of this technique, equipment, algorithms and results of experimental measurements are explained. In Section 4, the results from GPR are described: introduction, equipment, measurement and results. Finally, in Section 5 the main conclusions are listed.

2. Single hard wall waveguides

At historic walls, different typologies exist but brick walls, ashlar walls and rubble wall are the main ones (Figure 1). The first case was built mainly with cooked bricks as base material plus plaster or mortar as binding material. The bricklaying method could follow different pattern bonds: running, common or American, Flemish, English, stack, and English cross or Dutch bond. Ashlar walls and rubble walls masonry use same base material, ashlars of marble, but in case of masonry, the elements are more irregular and the wall has less compression resistances.

At this work, scale ashlar walls were made at laboratory facilities in order to be able to reproduce and to have control over the defects. Two walls (wall 1 and wall 2) were built with travertine ashlars from Godella's quarry (SPAIN) and the dimension of the ashlars was 40x30x20cm. The final dimension of the two walls was 287cm length, 220cm height and 20cm thickness. As binding material it was used impoverished mortar that has a low compression resistance (<4MPa), typical of historic buildings.

The two walls were divided in 7 rows, 4 of these rows are subdivided in 7 columns and the other 3 in 6 columns in order to have the intersection between rows and columns in the center of the ashlar (Figure 2). The separation between rows was 31cm and 41cm for columns. An ultrasonic measure has been taken (46 points per wall) per each point of this array providing a first tomography of the wall. Wall 1 was homogeneous

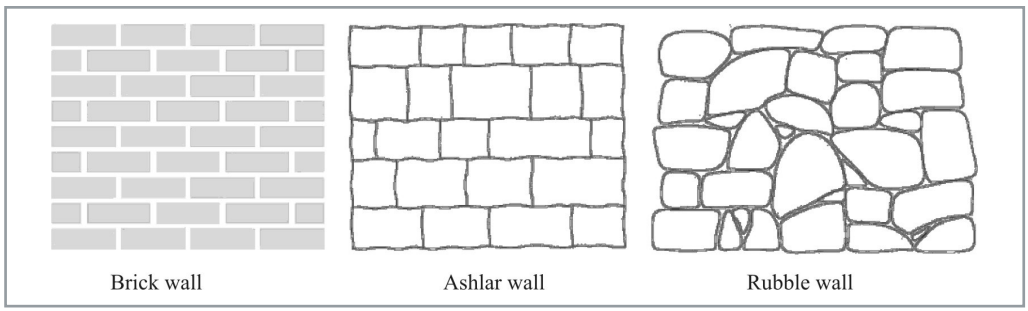

Figure 1. *Different kind of walls*

Figure 2. *Photography of ashlar wall (Wall 2)*

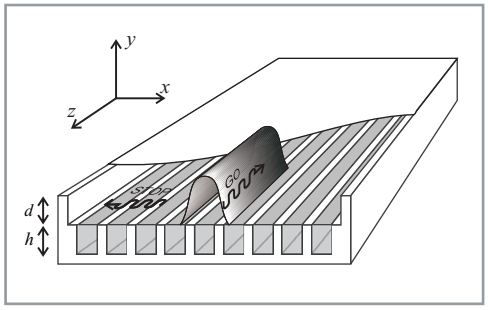

Figure 3 *Distribution of measurement positions and defects (Wal 2)*

whereas wall 2, some defects were artificially included: two drill holes, one vertical flaw and one crack or nook filled with mortar (Figure 3). The objective is to detect these defects by means NDE combined with signal processing algorithms. By other hand, the walls were introduced in a hydraulic press and were load with different levels of weight (10Tn, 50Tn and 80Tn) in order to check also the sensibility of the NDE to tensional state of the wall.

3. Ultrasonic testings

3.1 Introduction and hardware description

Non-destructive evaluation (NDE) by ultrasounds is a very useful technique that has been applied in several fields such as construction, food, and biomedicine. The technique has basically two operation modes: pulse-echo (one sensor is used both as emitter and as receiver) and through-transmission (two sensors are used, one emitter and one receiver sensor) [6]. An ultrasound pulse is injected in the inspected material and a response of the material structure is received. The measured signal can contain echoes produced from discontinuities, inhomogeneities, borders of the material, plus material grain noise (superimposition of many small echoes due to the material microstructure). All of this information can be used for quality control and characterization of materials since physical properties of the material such as porosity and density have a definite influence on the propagation of the ultrasound [7][8]. Recently, we introduced ultrasound NDE in novel applications to heritage problems: diagnosis of the consolidation condition, detection of layers in historical walls [9][10][11] and cataloguing of archaeological ceramics [12].

The hardware that has been used for ultrasonic measurements are composed by five modules: ultrasonic module, responsible of electric signal generation and conditioning (MATEC PR5000), acquisition module, responsible to digitalize electric signals (oscilloscope Tektronix 3012), control module (notebook), responsible to control other modules and process and store signals, transducer module, responsible to convert electric signals to ultrasonic signals and vice versa (1MHz K1SC from General Electrics) and finally an external pre-amplifier to provide an extra gain of 40dB. In Figure 4 it is shown photography of this equipment whereas in the Table 1 it is shown the setup parameters.

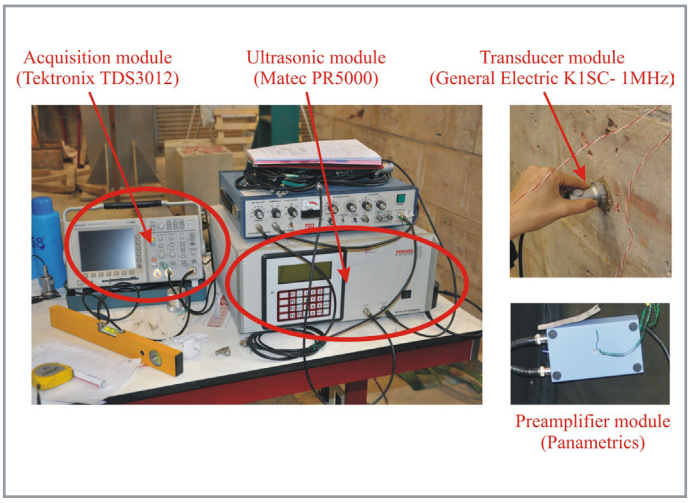

Figure 4. *Photography of ultrasonic equipment*

The variation of the color in the ultrasonic tomography provide information of the defect and spatial position

	Parameter	Value
Ultrasound parameters	Mode	Through/transmission
	PRF	76Hz
	Width	1μs
	Frequency	1MHz
	Amplitude	90%
	Gain	45dB+40dB
	Filter	[100kHz, 5MHz]
Acquisition parameters	Sample freq.	50MHz
	Bits/sample	12 real bits
	Sensibility	0.5V/div
	Dinamic range	8Vpp

Table1. *Setup parameters*

3.2 Ultrasonic signal processing

An ultrasonic measure (A-SCAN, Figure 5) has been taken for each spatial position described in Figure 2 and Figure 3. Beginning from these A-SCANs, different ultrasonic parameters are extracted and associated to each position. The selected parameters are speed (1), power (2) and maximum frequency (3) and have been selected due to their low variance. The temporal window used for their estimation begins at 30μs and finish at 100μs (Figure 5).

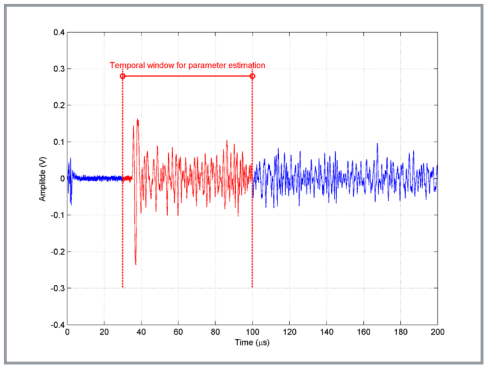

Figure 5. *Ultrasonic A-Scan*

$$V = \frac{Distance}{\text{Time of flight}} = \frac{d}{\Delta t} \tag{1}$$

$$P = \frac{\sum_{N_{Samples}} |x[n]|^2}{50 N_{Samples}} \tag{2}$$

$$f_{\max}[Hz] = \max_{f}\left\{X_{N_{samples}}(f)\right\}$$
$$X_{N_{samples}}(f) = TF\left\{x_{N_{samples}}(n)\right\}$$
$$x_{N_{samples}}(n) \rightarrow N_{samples} \text{ truncated from } x(n) \tag{3}$$

Once the ultrasonic parameters are extracted for each ashlar (Figure 2), it is possible to obtain an image or tomography where X axis is associated to the length and Y axis is associated to height of the wall. The color of the image represents the value of the selected parameter (Figure 6). Then, the variation of the color provide variation of the ultrasonic parameters that it is related to defect and spatial position.

As it is shown in Figure 6.a, the 46 measures do not provided smoothed tomographies and the heterogeneities (see the bottom right zone of the Figure 6.a) present sharp edges. It is necessary to apply interpolation algorithms to obtain a more realistic visualization of the tomography of the wall. For this case, it has been used a linear algorithm based in kriging. This algorithm predicts the value of unknown points, $\hat{Z}(r)$, as a linear combination from the known values $(Z(\boldsymbol{r}_{-i}))$ (1), where $\boldsymbol{r}$ is the position vector. Thus [13],

$$\hat{Z}(\mathbf{r}) = \sum_{i=1}^{N} Z(\mathbf{r}_i) W_i(\mathbf{r}) \tag{1}$$

The estimation of the weights $W_i(r)$ produces that the estimator for the interpolated values $\hat{Z}$ has an optimal relationship with a given set of N data values $Z(r_i)$, $i=1...N$. The restrictions that $E[\hat{Z}(\boldsymbol{r})\text{-}Z(\boldsymbol{r})]=0$ and the residual variance $\sigma_e^2 = \mathrm{E}\left[\left(\hat{Z}(\mathbf{r}) - Z(\mathbf{r})\right)^2\right]$ is minimum, impose the condition that the estimator is both unbiased and gives the least dispersion. Kriging established the concept of structural analysis, and the weight vector $W_i(\boldsymbol{r})$, , is estimated beginning from covariance and semivariogram which indicates the degree of correlation between values of the variable as a function of distance. The relevant definitions to kriging are the covariance (C) and the semivariogram (γ), defined by (4) and (5) respectively.

Generally, the covariance and the variogram depend on both positions r_1 and r_2, but in such a case many realizations of the pair are required to be evaluated. The hypothesis of stationarity has to be invoked involving to make the assumption that C and γ depend only on the separation vector $|\boldsymbol{r}_i\text{-}\boldsymbol{r}_j|$. This allows the consideration of all data points separated by the same distance, h, as being realizations of the same pair of the random variables $[Z(r_1)\text{-}Z(r_2)]$. Simple kriging obtains the weights $W_i(\boldsymbol{r})$ by solving the system of equations (6) and ordinary kriging solving the system equations (7) where μ is a Lagrange multiplier involved in the minimization of σ_e^2.

3.3 Ultrasonic results

The extraction and interpolation algorithms allow obtaining tomographies with a major number of points and improving the visual representation. In Figure 6.a, the original tomography is represented with a 7x7 grid. This tomography corresponds to wall 1, where a reduction of velocity could be appreciated in the right

$$C(\mathbf{r}_1, \mathbf{r}_2) = E[(Z(\mathbf{r}_1) - E[Z(\mathbf{r}_1)])(Z(\mathbf{r}_2) - E[Z(\mathbf{r}_2)])] \tag{4}$$

$$\gamma(\mathbf{r}_1, \mathbf{r}_2) = var\{Z(\mathbf{r}_1) - Z(\mathbf{r}_2)\}/2 \tag{5}$$

$$\begin{bmatrix} C(\mathbf{r}_1, \mathbf{r}_1) & \cdots & C(\mathbf{r}_1, \mathbf{r}_N) \\ \vdots & \ddots & \vdots \\ C(\mathbf{r}_N, \mathbf{r}_1) & \cdots & C(\mathbf{r}_N, \mathbf{r}_N) \end{bmatrix} \begin{bmatrix} W_1(\mathbf{r}) \\ \vdots \\ W_N(\mathbf{r}) \end{bmatrix} = \begin{bmatrix} C(\mathbf{r}_1, \mathbf{r}) \\ \vdots \\ C(\mathbf{r}_N, \mathbf{r}) \end{bmatrix} \tag{6}$$

$$\begin{bmatrix} \gamma(\mathbf{r}_1, \mathbf{r}_1) & \cdots & \gamma(\mathbf{r}_1, \mathbf{r}_N) & 1 \\ \vdots & \ddots & \vdots & 1 \\ \gamma(\mathbf{r}_N, \mathbf{r}_1) & \cdots & \gamma(\mathbf{r}_N, \mathbf{r}_N) & 1 \\ 1 & 1 & 1 & 0 \end{bmatrix} \begin{bmatrix} W_1(\mathbf{r}) \\ \vdots \\ W_N(\mathbf{r}) \\ \mu \end{bmatrix} = \begin{bmatrix} \gamma(\mathbf{r}_1, \mathbf{r}) \\ \vdots \\ \gamma(\mathbf{r}_N, \mathbf{r}) \\ 1 \end{bmatrix} \tag{7}$$

bottom of the image due to natural heterogeneities of the ashlars. This representation does not look natural and it is difficult to have an idea about the shape of the defect. Whereas, Figure 6.b represents the same tomography but with a 100x100 grid estimated by means ordinary kriging. Notice how visualization has improved and the shape of the defect can be appreciated clearly.

Once the interpolation and parameters extraction algorithms were implemented, it was checked the capacity of ultrasound for detecting the defects at ashalar wall 2, described in section 2. At first sight, the tomography did not show the defects. The variations of the tomography values that were expecting to associate with defects, were masked by variations of the own material and by the variance of the measurement. We can see in Figure 7 as speed varies, but these variations are not significant and do not correspond with the theoretical positions of defects. As several tomographies were obtained for different weights of load (see section "2. Description of scale ashlar masonry wall"), it was possible to obtain differential tomographies between loads. By this way, the variations between the ultrasonic parameter and the variations of the load were compared (ultrasonic parameters are sensible to tensional state: velocity and signal power suffer an increment with load whereas central frequency is kept constant). The result is shown in Figure 8, where it is important to notice how some defects are detected. The reason is that ultrasonic dependence with load is different between sound and unsound zones and ultrasonic parameters suffer different percentage of variation, as it is reflected in Figure 8. The vertical flaw and horizontal drill hole were not detected because the load was not so high to suppose an important variation of the ultrasonic parameter, in this case, velocity. The crack is perfectly detected by this way and it is possible to notice how this defect affects adjacent ashlars.

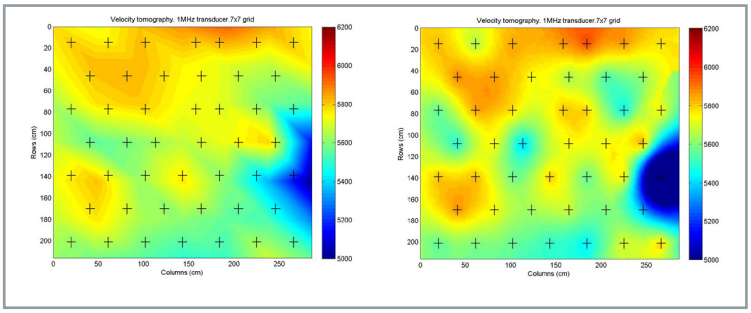

Figure 6. *Velocity tomographies (m/s) in ashlar wall 1. Different interpolation resolution: a) 7x7 b) 100x100*

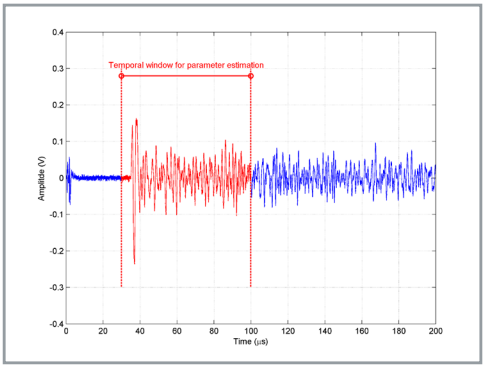

Figure 7. *Velocity tomography for Wall 2 with defect representation (m/s)*

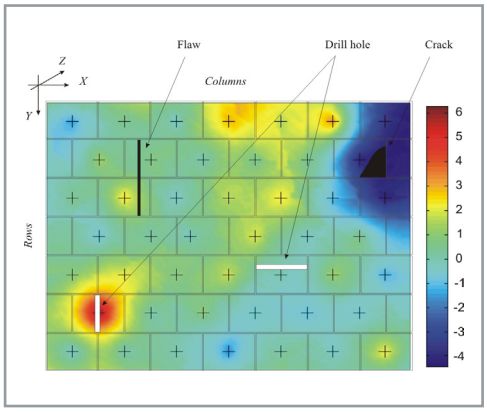

Figure 8. *Differential tomography of velocity (percentage of variation) for Wall 2 between weights of load (50Tn and 10Tn).*

4. Ground penetrating radar

4.1 Introduction and hardware description

Ground Penetrating Radar (GPR) is a Non-Destructive Evaluation (NDE) method that uses electromagnetic waves to study the composition of a material. The GPR equipment transmits pulses of radio waves through the material structure. Afterwards, the response of the material is measured by signals that contain the reflections produced by the microstructure plus the echoes caused by the inhomogeneities inside the material [14][15]. The principal goal of the GPR signal processing consists of characterizes the propa-

Figure 9. *Photography of GPR SIR 3000 with 1.6GHZ antenna plus displacement device*

Figure 10. *Realization of GPR measurement*

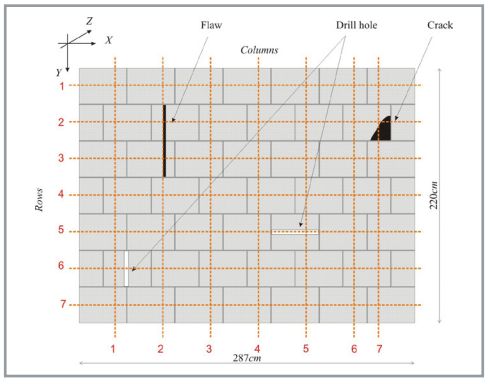

Figure 11. *Description of GPR trayectories*

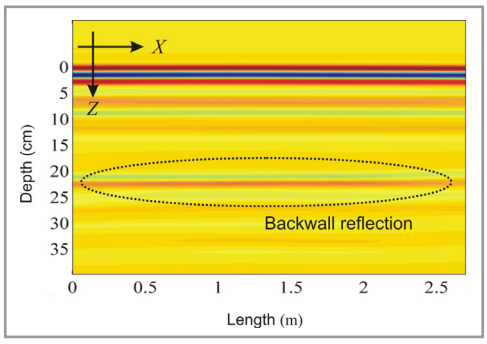

Figure 12. *Example of radargram*

gation medium and then subtracting it from the measured signals in order to detect the material inhomogeneities. GPR has been used in several applications such as detection of non-metallic land mines; concrete and rebar imaging and inspection; and locating unmarked geologic sites of interest [16][17]. However, there are a few references of application of GPR in historic buildings NDE [18][19].

The used equipment was a SIR 3000 from "Geophysical Survey Systems, Inc" with 1.6GHz antenna. The dimension of the antenna was 3.8x10x16.5 cm and it was fit to an encoder displacement device (Figure 9). Figure 11 represent the positions and trayectories that have been measured with GPR to obtain the radargrams. A radargram is an image (also called B-Scan) that represents values of the measured signal at different depths of the material through the points of a trajectory; see an example in Figure 12. The horizontal axis of this radargram represents the position of the antenna along a row or column, whereas the vertical axis represents the penetration of the electromagnetic wave, it means the width of the wall. And finally, the level of signal is presented in pseudo-color. By this way and beginning from this radargram, it is possible to obtain information about the width of the wall, the presence or not of faults and material changes and the positions of these artifacts. In Figure 12, it is possible to see the backwall reflection or echo and therefore to determine the depth of the wall. It is important to notice, that these radargram differs from ultrasonic tomographies. The ultrasonic tomography provides a kind of frontal radiography of the wall. Whereas, the radargram provides information from a cut of the wall.

As it is shown Figure 11, the wall was divided in 7 columns and 7 rows of 2.2m and 2.87m respectively. The setup of the equipment was distance mode with 156 scans per meter. It means 343 scans for each column and 447 scans for each row. The acquired time for each scan was 10ns. A temporal scan is shown in Figure 10 and beginning from this register, the dielectric constant $(\varepsilon_r, wall)$ was calculated (8) for the wall. Beginning from this $\varepsilon_r, wall$, the propagation velocity of the wall, $v_p, wall$, is derived and the temporal axis converts into distance axis.

$$\Delta z = 20.4cm \rightarrow \text{Distance}$$

$$c = 3{\cdot}10^{10}\, cm/s \rightarrow \text{Light velocity}$$

$$T = \frac{10ns}{1024} = 9.76\, ps \rightarrow \text{Sampling frequency}$$

$$N_{muestras} = \left(426 - \frac{197}{2}\right) = 328 \rightarrow \text{Samples associated to } \Delta z$$

$$\varepsilon_{r,muro} = \left(\frac{c\frac{T}{2}N_{muestras}}{\Delta z}\right)^2 = 5.55 \rightarrow \text{Dielectric constant of wall}$$

$$v_{p,wall} = \frac{c}{\sqrt{\varepsilon_{r,muro}}} = 2.345{\cdot}10^{10}\, cm/s \rightarrow \text{Wall velocity}$$

(8)

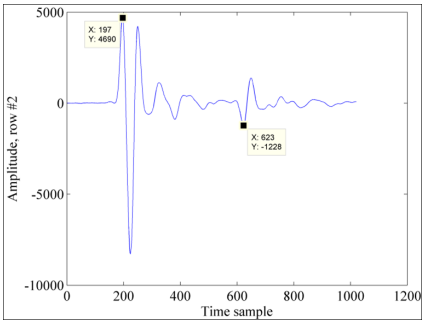

Figure 13. *A-scan used for calculation of the dielectric constant of the material*

4.2 GPR signal processing

As it has explained, a radargram is an image that represents values of the measured signal at different depths through a trajectory. The objective of the several processing steps is to highlight the zones in the radargram where the inhomogeneities are located. The GPR signal processing has been implemented in three main stages: background signal removal, depth resolution enhancing and Kirchoff migration; see Figure 14.

The first stage, background signal removal, assumes that the measured GPR signal is a mixture for blind source separation (BSS) using independent component analysis (ICA). This technique aims to separate hidden sources from their observed linear mixtures without any prior knowledge [20]. Thus, ICA was applied to separate the background (reflections from the air-wall interfaces) from the rest of the backscattered measured signal. The background contributes to the observed mixture (the GPR signal) as a kind of interference that is recovered by ICA. We assumed that the signal of backscattering measured by the GPR can be modelled as a stochastic process $\{Z(x,t)\}$, with x being the position and t the time [10]. This model can be written as: $\{Z(x,t)\} = \sum_{n=1}^{N(x)} A_n(x) f(t-\tau_n)$, where A_n is the scattering cross-section of the n-th scatter at position x, τ_n is the delay of the backscattered signal, and $N(x)$ is the number of scatterings that contribute from position n.

A novel ICA algorithm called Mixca was applied for background signal removal [12]. This algorithm provides several advantages over classical ICA algorithms such as increasing of the source modelling flexibility since the probability density functions of the sources are modelled with non-parametric distributions. In addition, the system includes two additional classical methods for background removing (polynomials and spatial mean) and several methods to enhance the captured data such as depth resolution enhancement, and cepstral deconvolution [21][22][23].

The second stage, resolution enhancement, is implemented by means an AGC (Automatic Gain Control) button to enhance contrast [24] and an

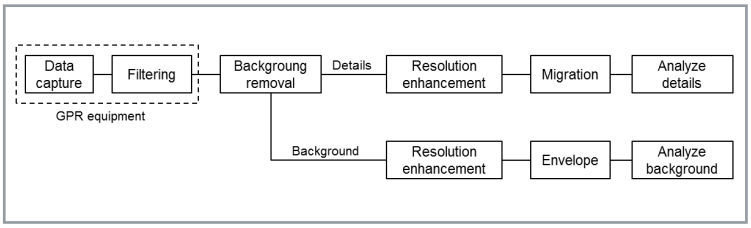

Figure 14. *Stages of data processing method*

envelope button, which shows the time envelope of the most recent result (sometimes used for data interpretation). Finally, the third stage, Kirchoff migration, tries to correct the effect of the antenna radiation diagram. This effect produces that a punctual reflector becomes into a hyperbola. These hyperbolas have been detected using Hough transformed and Random Hough transform and have been corrected using the Kirtchoff method. At Figure 15, it is shown the result of this stage and how the hyperbola is returned to a more realistic shape.

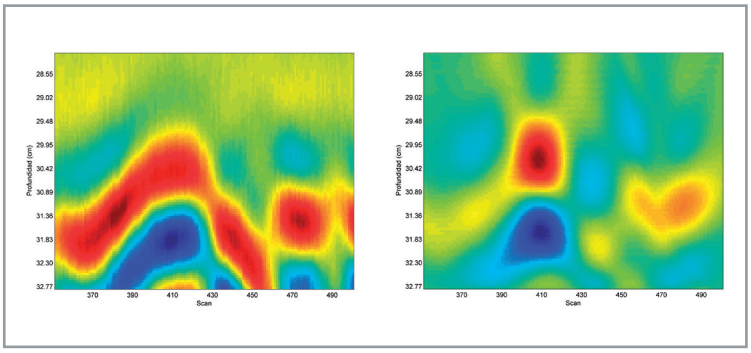

Figure 15. *Migration example: a) Direct radargram (the reflector produces a hyperbola). b) Radargram after migration process*

4.3 GPR Results

Many of the flaws described in Figure 3 were detected. Fig. 12 shows the obtained results where the crack and the flaw that are on row 2 are detected. Notice the difference in perceived amplitude between both defects. Said difference is due to the straight geometry of the flaw, which accentuates the reflection of the waves. The crack is irregularly shaped and with rough

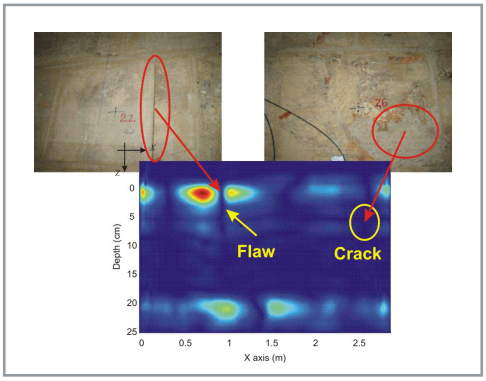

Figure 16. *Flaw and crack detection in masonry wall 2:*

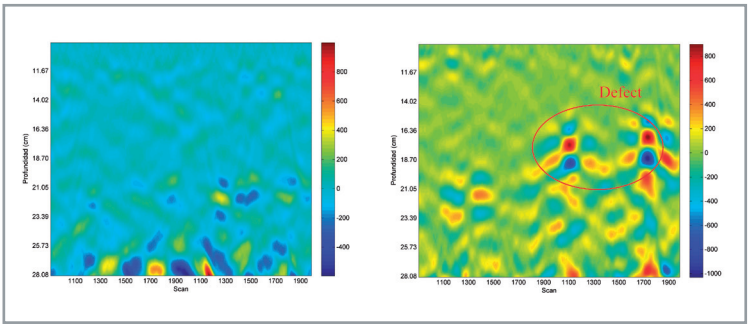

Figure 17. *Radargrams for different loads (row 5): a) Preload, b) 50 Tn.*

faces, and thus scatters incident waves and so received signal values for that position are lower than those measured at the location of the flaw.

Additionally, it is important to notice that the detection results were better for high load values. The reflection of incident waves from the flaws is strengthened with the increase in compression, allowing for a better definition in the radargrams of the shapes of the imperfections. Figure 17 shows how the horizontal B-Scan varies with the increase of the load and the detection of the defect is enhanced.

5. Conclusions

The proposed approach for the auscultation of historical masonry walls with ultrasound and ground-penetrating radar (GPR) has proved to be effective for the detection of flaws and cracks and the characterization of walls under load. It was possible to detect flaws with a size of millimeters and variations in the interfaces between ashlars and mortar caused by effect of the compression suffered under load.

Ultrasonic tomographies and radargrams are techniques that allow representing the internal structure of walls. Nevertheless, inhomogeneities inside the walls will be more or less visible due to their geometry, orientation and physical properties (especially their contrast with the surrounding medium). Because of this, adaptive processing techniques are required to successfully show the different defects. In the case of ultrasonic, different parameters have been estimated with low variance algorithms and differential tomographies have shown their capability. Additionally, linear interpolation algorithm has been implemented for visual enhacement. In the case of GPR, novel algorithm have been developed to remove the background signal and to enhance spatial resolution.

Acknowledgements

This work has been supported by the Generalitat Valenciana under grant PROMETEO/2010/040

References

[1] D. Watt, Building Pathology: Principles and Practice, 2nd Edition, Wiley-Blackwell, 2007.

[2] D. Friedman, Historical Building Construction: Design, Materials, and Technology, 2nd Edition, W. W. Norton & Company, 2010.

[3] B. Middendorf, J.J. Hughes, K. Callebaut, G. Baronio, I. Papayianni, Investigative methods for the characterisation of historic mortars - Part 1: Mineralogical characterisation, Materials and Structures/Materiaux et Constructions, vol. 38 no. 282, pp. 761-769, 2005.

[4] B. Middendorf, J.J. Hughes, K. Callebaut, G. Baronio, I. Papayianni, Investigative methods for the characterisation of historic mortars - Part 2: Chemical characterisation, Materials and Structures/Materiaux et Constructions, vol. 38 no. 282, pp. 771-780, 2005.

[5] A. Salazar, L. Vergara, L., R. Llinares, R, "Learning material defect patterns by separating mixtures of independent component analyzers from NDT sonic signals", Mechanical Systems and Signal processing, vol. 24 no. 6, pp. 1870-1886, 2010.

[6] J. Krautkrämer, Ultrasonic Testing of Materials, Springer, 4th edition, Berlin, 1990.

[7] M. Sansalone, W. Street, Impact-Echo: Nondestructive evaluation of concrete and masonry, Bullbrier Press, New York, 1997.

[8] J.D. Cheeke, Fundamentals and Applications of Ultrasonic Waves, CRC Press LLC, USA, 2002.

[9] J. Gosalbez, A. Salazar, I. Bosch, R. Miralles, L. Vergara, "Application of ultrasonic nondestructive testing of consolidation of a restored dome", Materials Evaluation, vol. 64 no. 5, pp. 492-497, 2006.

[10] A. Salazar, J. Gosálbez, J. Igual, R. Llinares, L. Vergara, "Two applications of independent component analysis for non-destructive evaluation by ultrasounds", Lecture Notes in Computer Science, vol. 3889, pp. 406-413, 2006.

[11] L. Vergara, I. Bosch, J. Gosalbez, A. Salazar, "Optimum detection of ultrasonic echoes applied to the diagnosis of the first layer of a restored dome", Journal of Advances in Signal Processing, vol. 2007, Article ID 26560, 10 pages, doi:10.1155/2007/26560, 2007.

[12] A. Salazar, L. Vergara, "ICA mixtures applied to ultrasonic nondestructive classification of archaeological ceramics", Journal on Advances in Signal Processing, vol. 2010, Article ID 125201, 11 pages, doi:10.1155/2010/12520, 2010.

[13] L.M. Surhone, M.T. Timpledon, S.F. Marseken, Spatial Descriptive Statistics: Descriptive Statistics, GIS, Geostatistics, Variogram, Correlogram, Kriging, Cuzick-Edwards Test. Betascript Publishing, 2010.

[14] D.J.Daniels, Surface Penetrating Radar. The Institution of Electrical Engineers, 1996.

[15] J. M. Reynolds, An Introduction to Applied and Environmental Geophysics. Wiley, 1997.

[16] P. K. Verma, A. N. Gaikwad, D. Sigh, M. J. Nigam, "Analysis of clutter reduction techniques for through wall imaging in UWB range", Progress In Electromagnetics Research B, vol. 17, pp. 29-48, 2009.
[17] J. H. Bungey, "Sub-surface radar testing of concrete: a review", Construction and Building Materials, vol.8, pp.1-8, 2004.
[18] C. Maierhofer, S. Leipold, "Radar investigation of masonry structures", NDT&E International, vol.34, pp.139-147, 2001.
[19] G. Safont, A. Salazar, J. Gosalbez, L. Vergara, "Intelligent system for non-destructive evaluation of historic walls using ground-penetrating radar", Proceedings of IEEE 9th International Conference on Cybernetic Intelligent Systems, CIS 2010, pp. 100-105, Reading, England, 2010.
[20] P. Comon, C. Jutten eds, Handbook of Blind Source Separation, Independent Component Analysis and Applications, Academic Press, 2010.
[21] P. Kennett, Geophysics. Longman, 1983.
[22] J. M. Reynolds, An Introduction to Applied and Environmental Geophysics. Wiley, 1997.
[23] L. Cedrina, N. Bonomo, and A. Osella, "An Application of the Synthetic Emitter-array Method to Improve GPR Signals," Journal of Applied Geophysics, vol. 70, no. 3, 237-344, 2010.
[24] O. Yilmaz, Seismic Data Processing. SEG Publishing, Tulsa, 1987.

Biographies

Dr. Jorge Gosálbez was born in Valencia (Spain) in 1975. He received Telecomunications Engineering and PhD degrees from the Universidad Politécnica de Valencia (UPV) in 2000 and 2004 respectively. He is Associate Professor at Departamento de Comunicaciones (UPV) and member of the Signal Processing Group of the Institute of Telecommunication and Multimedia Applications (I-TEAM) of UPV. His research concentrates in the statistical signal processing area, where he has worked in different theoretical an applied problems. His theoretical aspects of interest are time-frequency analysis, signal detection and array processing. Currently he is involved in ultrasound signal processing for non-destructive evaluation of materials, in surveillance systems based on acoustic information and in acoustic source location and tracking based on sensor and array signal processing. He has published more than 50 papers including journals and conference contributions.

Dr. Addisson Salazar received the B.Sc. and M.Sc. degrees in Information and Systems Engineering from Universidad Industrial de Santander, the D.E.A. degree in Telecommunications from Universidad Politécnica de Valencia (UPV) in 2003, and the Dr. in Telecommunications degree from UPV in 2011. He obtained the Accreditation to Associate Professor from the Comisión Valenciana de Acreditación y Evaluación de la Calidad in 2005. Since 2002, he has been with the Signal Processing Group in the Institute of Telecommunications and Multimedia Applications at UPV where he was appointed as an official scientific staff member in 2007. His research interests include statistical signal processing, machine learning, and pattern recognition with emphasis on methods for signal classification based on time-frequency techniques, blind source separation and mixtures of independent component analyzers. The application of his research has been focused on nondestructive testing and biomedical problems.

MSc. Gonzalo Safont was born in Madrid (Spain) in 1985. He received the Telecommunications Engineering degree from the Universidad Politécnica de Valencia (UPV) in 2008. He is currently a Ph.D. student in the Institute of Telecommunication and Multimedia Applications (I-TEAM) of UPV. His research concentrates on the statistical signal processing area, where he has worked with several theoretical and applied problems. His theoretical aspects of interest are statistical signal processing and pattern recognition, with emphasis on blind source separation and mixtures of independent component analyzers. Currently he is involved in ground-penetrating radar data processing for non-destructive evaluation of materials.

Dr. Ignacio Bosch was born in Valencia (Spain) in 1975. He received Telecomunications Engineering and PhD from the Universidad Politécnica de Valencia (UPV) in 2001 and 2005 respectively. In 2004 he became a lecturer in the Departamento de Comunicaciones. From 2006 until now he has been working as an Assistant Professor at the Escuela Politécnica Superior de Gandia. He is member of the Institute of Telecommunication and Multimedia Applications (I-TEAM) of UPV. He

is responsible of developing algorithms and systems for infrared signal processing surveillance. His research interests are signal processing applications for ultrasonic systems in non-destructive evaluation and infrared signal processing for automatic fire detection. He has been actively participating in forty-four research projects and/or research contracts. He has published more than 60 papers including journals and conference contributions.

Dr. Ramon Miralles was born in Valencia (Spain) in 1971. He received Telecomunications Engineering and PhD degrees from the Universidad Politécnica de Valencia (UPV) in 1995 and 2000 respectively. In 1996 he became a lecturer in the Departamento de Comunicaciones at the Escuela Politécnica Superior de Gandia. From 2000 until now he has been working as an Assistant Professor in the Escuela Tecnica Superior de Ingenieros de Telecomunicación (Valencia). He is member of the management team of the Institute of Telecommunication and Multimedia Applications (I-TEAM). He is co-author of more than 22 journal papers and 50 international conferences. His main research interests include higher order statistics, nonlinear signal processing and signal processing applications for ultrasonic systems.

Prof. Luis Vergara was born in Madrid (Spain) in 1956. He received the Telecomunications Engineering and PhD degrees from the Universidad Politécnica de Madrid (UPM) in 1980 and 1983 respectively. Until 1992 he worked at the Departamento de Señales, Sistemas y Radiocomunicaciones (UPM) as an Associate Professor. In 1992 he joined the Departamento de Comunicaciones (Universidad Politécnica de Valencia UPV, Spain), where he became Professor and where it was Department Head until April 2004. From April 2004 to April 2005 he was Vicerector of New Technologies at the UPV. He is now responsible of the Signal Processing Group of the UPV, a member group of the Institute of Telecommunication and Multimedia Applications (I-TEAM) of UPV. His research concentrates in the statistical signal processing area, where he has worked in different theoretical an applied problems. His theoretical aspects of interest are signal detection and classification, independent component analysis and spectral analysis. Currently he is involved in ultrasound signal processing for non-destructive evaluation, in infrared signal processing for fire detection and in cognitive audio for surveillance applications. He has published more than 150 papers including journals and conference contributions.).

MSc. Vicente Albert Pérez was born in Valencia (SPAIN) in 1981. He received the Telecommunications Engineering degree in 2007 from Universidad Politécnica de Valencia (UPV). In 2008 received a Master of Science in the field of technologies, systems and communications networks in Department of Communications at UPV. Currently, he is a PhD student in Department of Communication at UPV since 2008. From 2005, he works as technician in structural health monitoring and electronics development in AIDICO-Technological Institute of Construction. Until now he has more than 10 conference papers in the field of monitoring techniques in civil engineering and heritage buildings. His research focuses on static and dynamic monitoring, digital signals processing and electronic devices development and is funded by regional, national and European programs.